Microscopic and mechanical properties of semi-crystalline and amorphous polymeric parts produced by laser cutting

Ayub Karimzad Ghavidel, Mohammadreza Shabgard, Hasan Biglari

Department of Mechanical Engineering, University of Tabriz, Iran, Tabriz
Correspondence to: A. Karimzad Ghavidel (E-mail: st_a.karimzad@urmia.ac.ir or ayobkarimzad@gmail.com)

ABSTRACT: Microscopic and mechanical properties of polymeric parts are effective factors on their durability. Laser cutting is one of the most common methods for production of 2D polymeric parts. Experimental study of the mentioned properties of semi-crystalline and amorphous polymeric parts after laser cutting is conducted in this research. Low density polyethylene (LDPE) and polystyrene (PS) are considered as semi-crystalline and amorphous polymers, respectively. Laser power and cutting velocity were selected as input parameters of cutting process. According to microscopic observations, the microcracks, re-solidified spots of molten material, and sink marks just appear in heat affected zone (HAZ) on amorphous polymer. Results also showed that the HAZ width and surface roughness values are smaller for semi-crystalline polymer. For both polymers, decreasing of power and increasing of cutting velocity reduce the HAZ and surface roughness. In the case of mechanical properties, tensile strength of semi-crystalline and amorphous polymers reduces after laser cutting. Results of experiments revealed that the extension of HAZ and deterioration of surface finish decrease tensile strength of parts. Therefore, lower power and higher cutting velocity condition is preferable for reaching the better mechanical properties. Furthermore, two separate mathematical models for each polymer are presented for prediction of tensile strength after laser cutting process. © 2016 Wiley Periodicals, Inc. J. Appl. Polym. Sci. **2016**, *133*, 44179.

INTRODUCTION

Laser cutting is a very common method in order to produce 2D polymeric parts.[1] Electronic and aerospace industries can be mentioned as major consumers for produced parts by this method.[2] Heat affected zone (HAZ), surface roughness, accuracy of dimensions, height of burr, and shape and width of kerf are considered the main output parameters of laser cutting process.[1,3] These outputs are mainly depended on thermal and optical properties of parts.[4,5] Many different polymeric materials and their composites were cut by different type of lasers and the mentioned outputs were studied on them.

Caiazzo *et al.* preformed laser cutting of polycarbonate (PC), polypropylene (PP), and polyethylene (PE). The comparison between obtained results showed that the taper angle of kerf for PE samples was bigger.[6] Acrylonitrile-butadiene-styrene (ABS) is a thermoplastic and its laser workability was evaluated by Shin *et al.* They proved that the increase of laser energy deepens the penetration of beam.[7]

Davim *et al.* in two different researches studied laser cutting of different polymeric materials. Outcome of their work was

introduction of poly(methyl methacrylate) (PMMA) and its composites as high potential polymer for laser cutting.[8,9] Also, Choudhury and Shirley studied surface roughness and burr on PMMA, PC, and PP .Their findings showed, in the case of PMMA, covering air pressure has the least effect on HAZ.[10] Recently, Niino *et al.* have studied laser cutting of carbon fiber reinforced plastic (CFRP)-ABS and CFRP-PPS (polypropylene sulfide) using high power laser. Favorable kerf by minimal taper angle was achieved with high speed. Higher cutting depth for CFRP-PPS samples in comparison with CFRP-ABS is other remarkable finding by these researches.[11]

Some other researchers used laser process for creation of new property on special polymer base material. Karimzad *et al.* reported new properties that can be generated using CO_2 laser on PMMA/multi-walled carbon nanotubes (MWCNT) nanocomposite. Accordingly, irradiation of laser beam in distinct path on PMMA/MWCNT nanocomposite can create electrical conductivity on the surface.[12]

Some papers investigated the influence of laser on mechanical and physicochemical properties. Lootz *et al.* studied the effect of laser cutting on morphological and physicochemical

Table I. The Characteristics of Used Materials

Property	Unit	Test condition	PS	LDPE
Yield tensile strength	Mpa	ASTM D638 (50 mm/min)	45	35
Elongation at break	%		5	50
Melt Flow Index (MFI)	g/10 min	ASTM D1238	9.3 (190°C/5 kg)	17.5 (190°C/2.16 kg)
Thermal conductivity	W/m K	ASTM D5930-09	0.14	0.36
Density	g/cm^3	ASTM D792-13	1.06	0.92
Specific heat	kJ/kg K	ASTM C351	1.20	2.30
Glass transition temperature	°C	ASTM D3418-15	101	−120
Melt temperature	°C	At room pressure	—	168
Thermal diffusivity	10^6 m^2/s	20°C	0.12	0.12
Coefficient of linear expansion	10^6 K^{-1}	ASTM D696-08	70	250

properties of polyhydroxybytyrate (PHB). They found that in the vicinity of laser cut edge the mechanical behavior changed from elastic to brittle. Alternation of the structural arrangement, reduction of molecular weight, and decreasing of the triethylcitrate (TEC) concentration were reported as reasons of this phenomenon.[13]

Herzog et al. studied the effect of production method of CFRP parts on tensile and bending strength. They utilized Nd: YAG, CO_2, and disk laser in their research. The results showed that tensile and bending strength of produced parts directly depend on the type of laser.[14]

The effect of the laser input parameters on mechanical and microscopic properties of amorphous and semi-crystalline thermoplastics are investigated in this research. In order to determine the relationship between laser cutting process and mechanical properties, the HAZ, surface roughness, and burr were studied as output parameters.

EXPERIMENTAL

Materials and Setup
The low density polyethylene (LDPE-Dupont6611) and polystyrene (PS-Chimi PH-88S) sheets produced by extrusion method (Aida plastic–co) were used during the experiments. The

mechanical and physical properties of these materials are presented in Table I.

Laser Cutting Process and Variables
Laser cutting of the samples were carried out on a laser cutting machine consisting of 120 W continuous wave (cw) CO_2 laser (Sahand Laser Technology) with a two axes numerically controlled table and dimensional limits of 1300 mm × 1000 mm. The compressed air was used as covering gas with 0.028 bar pressure. Focal point is fixed on the middle of work piece.[8] The cutting width of 0.1 mm was created by the utilized machine. Figure 1 shows the laser cutting process and the produced samples.

Three parameters, including the type of polymer (two types—polyethylene and polystyrene as semi-crystalline and amorphous thermoplastic, respectively), laser power (in four levels), and cutting velocity (in four levels), were considered as input variables of laser cutting process. These parameters and their levels are summarized in Table II. Full factorial method was selected for design of experiments (DOE) and each experiment was iterated for three times and the average values of measured features were reported for every run. The parameters were chosen in a logical way by testing so that it will make it possible to have a perfect cut through the parts and laser beam can penetrate

(a)   (b)

Figure 1. Laser cutting process and produced samples. [Color figure can be viewed in the online issue, which is available at wileyonlinelibrary.com.]

Table II. Levels of the Processing Parameters of this Research

Parameters	Levels of the processing parameters of this research levels				Symbol
Polymer type	LDPE		PS		T
Laser power (watt)	70	80	90	100	P
Cutting velocity (mm/s)	0.04	0.08	0.12	0.16	V

completely. It should be mentioned that due to the oriented properties of produced part by extrusion, the parallel ordination with extrusion direction was opted as study direction.

Characterization Process of Samples
Tensile properties of the parts were studied at strain rate of 10 mm/min for PS and LDPE samples according to the ASTM D638 at room temperature using Gotech (Al-7000M). Maximum loading capacity of this machine is 200 kN with precision of ±0.25%.

Olympus optic microscope was used for measuring the HAZ with magnification of ×200. In order to investigate the surface integrity of samples atomic force microscopy (AFM) system (Ara-Pajohesh) was employed before and after laser cutting. The disk micrometer with resolution of 10 μm (Mitutoyo, Japan) was utilized for measuring the height of burr. Ttr-220 surface roughness tester was also used according to ISO4288, with sampling length of 4.8 mm and cut off length of 0.8 mm.

In order to measure the cutting temperature in laser cutting process, Fluke VT04 visual IR thermometer was employed. All measurements were replicated three times for each part and subsequently the average values were reported as the response values.

RESULTS AND DISCUSSION

Morphology of Laser Cut Surface
The AFM images of samples before and after laser cutting are shown in Figure 2. As can be seen, the laser beam contact with PE samples did not have significant effect on the surface structure. However, for PS samples, it can be clearly seen that the contact of laser beam altered the surface conditions and the formation of microcracks on the surface is noticeable. The appearance of microcracks after laser cutting should be taken into account because it is an influential parameter on mechanical and surface properties. When the part having microcracks is loaded, the cracks will progress and eventually results in fracture
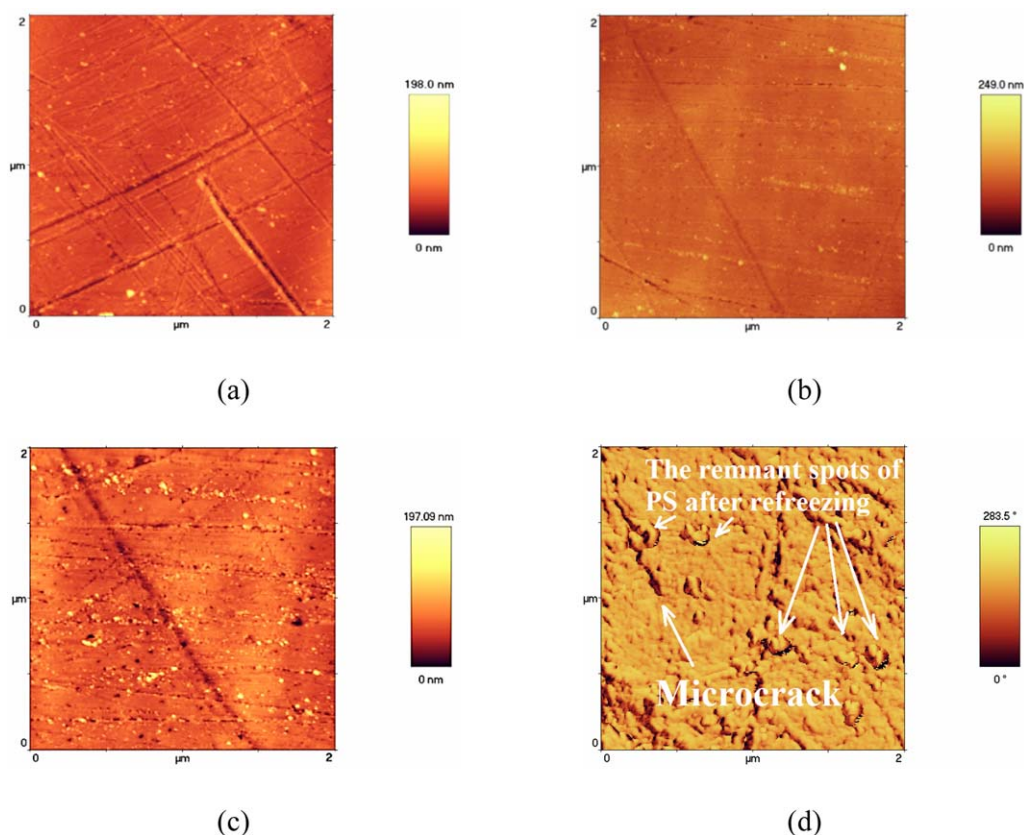

(a)

(b)

(c)

(d)

Figure 2. The AFM images of samples before and after laser cutting process (power 100 W and feed 0.04 m/min), (a,b) before and (c,d) after right column LDPE–left column PS. [Color figure can be viewed in the online issue, which is available at wileyonlinelibrary.com.]
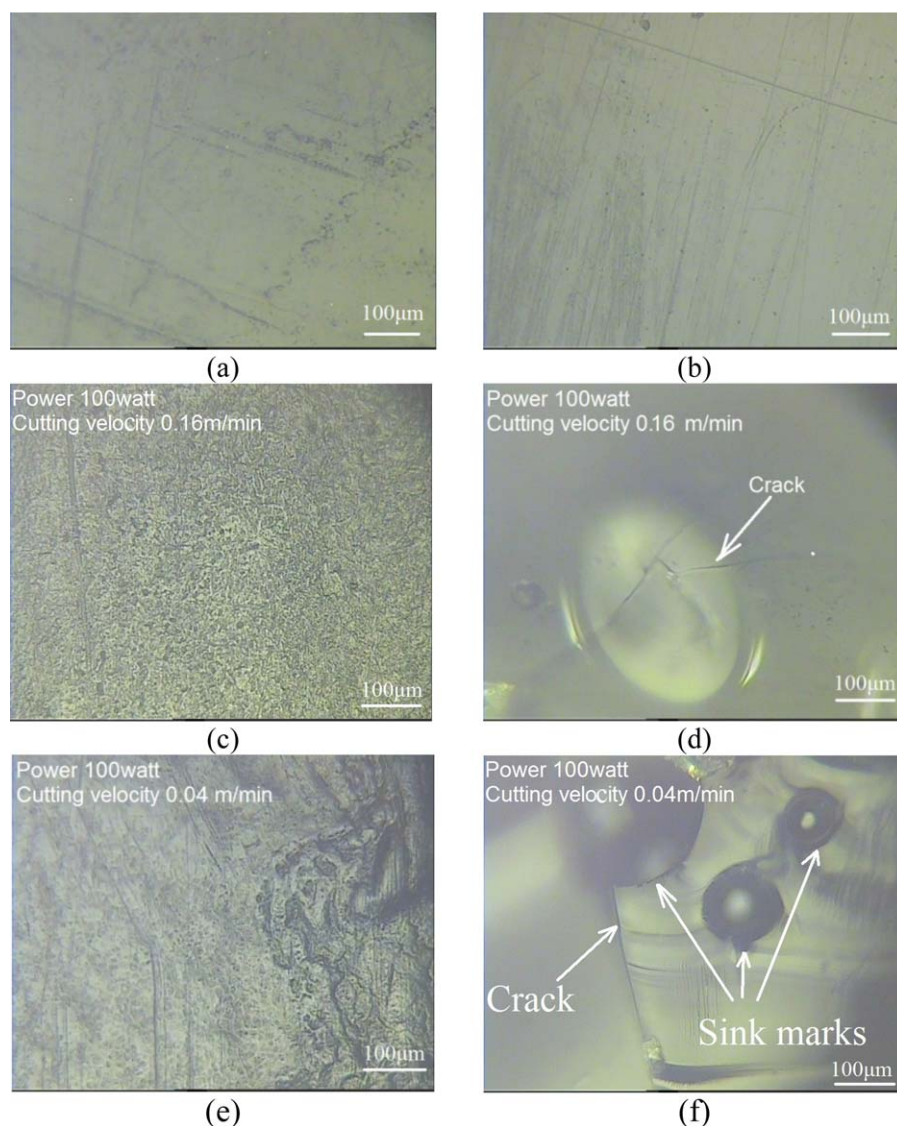
Figure 3. Microscopic images of specimens: left column LDPE–right column PS (a,b) before laser cutting and (c–f) after laser cutting. [Color figure can be viewed in the online issue, which is available at wileyonlinelibrary.com.]

of part under load. On the other hand, the spots of PS remained after laser cutting on the surface. This point shows that the micro-droplets of PS after melting can re-solidify rapidly, stick to surface, and create protruded spots on it. The presence of mentioned spots decreases the quality of surface and makes it rougher.
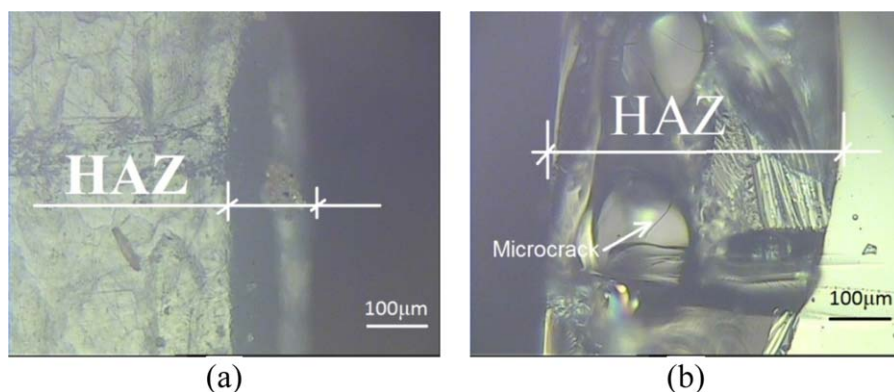

Figure 4. Microscopic images from HAZ—Power 100 W and cutting velocity 0.04 m/min (a) LDPE and (b) PS. [Color figure can be viewed in the online issue, which is available at wileyonlinelibrary.com.]
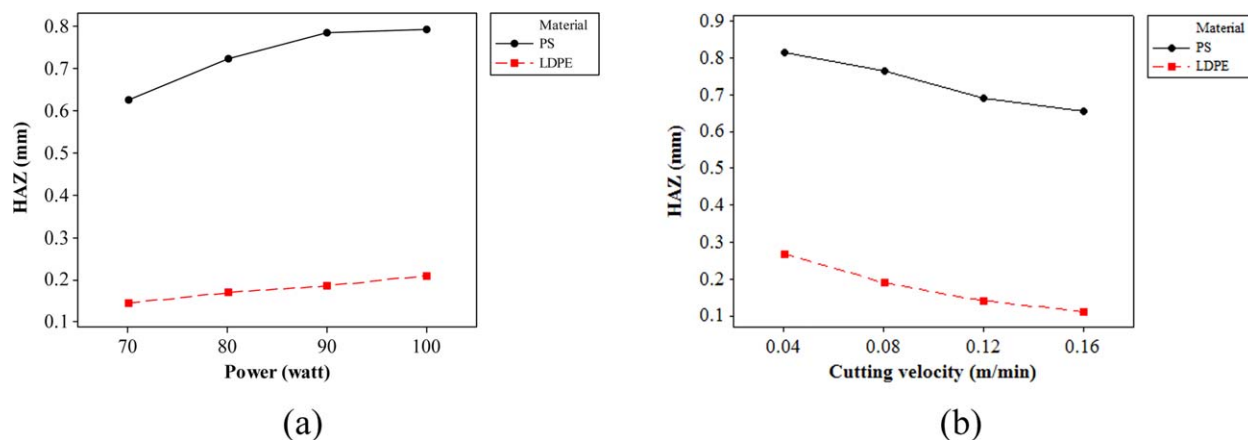
Figure 5. Influence of (a) power and (b) cutting velocity on HAZ. [Color figure can be viewed in the online issue, which is available at wileyonlinelibrary.com.]

In order to investigate the structure of surface after laser cutting in higher scale, they were examined by optical microscope. Figure 3 shows the microscopic images of cut surface of samples. According to this figure, cracks, sink marks, and also re-solidified spots can be seen on the PS samples while not observable on the PE samples. For better clarification of current observations, the thermal behavior of amorphous (PS) and semicrystalline (PE) polymeric material should be studied. The PS is an amorphous polymeric material and has the different behavior in melting phase and refreezing. The melting doesn't occur in the case of amorphous polymers. They just find fluency (melt-viscose) property by increasing temperature up to the glass transition temperature (T_g). This property causes to make hard the elimination of PS from the laser cutting path (kerf). Therefore, part of melted PS remains in the form of spots on the cut surface.

The most noticeable alternation in specific volume and mechanical properties occur at the T_g point. In laser cutting process of PS, the edges of cutting path experience T_g for two times and subsequently its alternations. First, when the temperature is increased by irradiation of laser beam and the second, when the melted material on cut edges re-solidifies. So, the defects like cracks and sink marks appear on the surface.
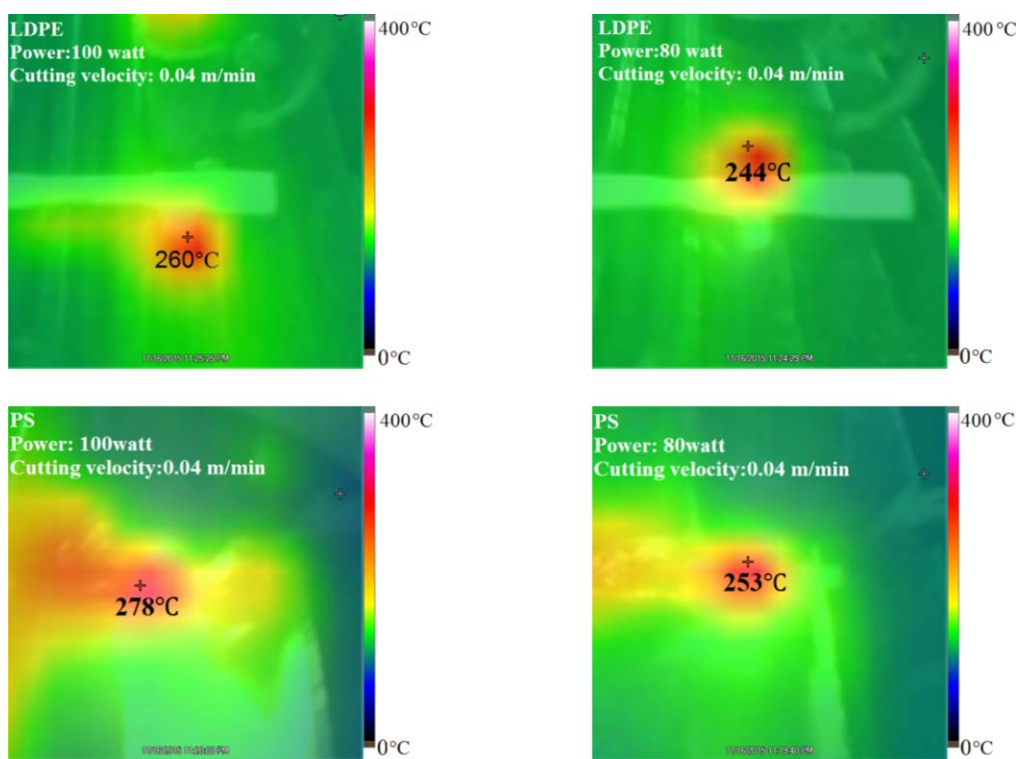

Figure 6. Thermal images from laser cutting of LDPE and PS. [Color figure can be viewed in the online issue, which is available at wileyonlinelibrary.com.]

Table III. Analysis of Variance of HAZ Results

Source	DF	Seq SS	Adj SS	Adj MS	F	P	P-effect	Statistical F
T	1	2.47114	2.47114	2.47114	8653.15	0.000	97.36	5.12
P	3	0.06359	0.06359	0.02120	74.22	0.000	0.84	3.86
V	3	0.11821	0.11821	0.03940	137.98	0.000	1.55	3.86
$T \times P$	3	0.01627	0.01627	0.00542	18.99	0.000	0.21	3.86
$T \times V$	3	0.00113	0.00113	0.00038	1.32	0.328	0.01	3.86
$P \times V$	9	0.00668	0.00668	0.00074	2.60	0.085	0.03	3.18
Error	9	0.00257	0.00257	0.00029				
Total	31	2.67960			$S = 0.0169$ R-Sq $= 99.89\%$ R-Sq(adj) $= 99.67\%$			
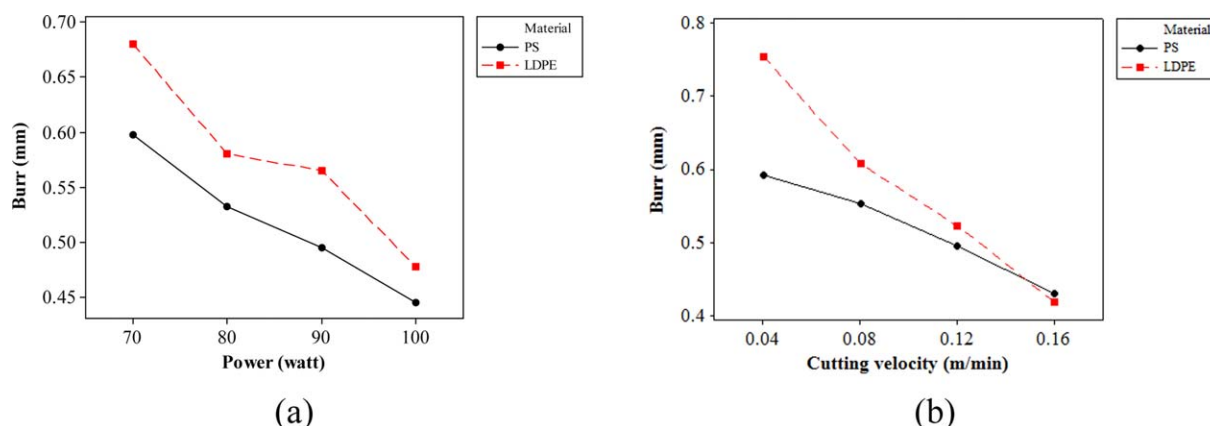
Figure 7. Influence of (a) power and (b) cutting velocity on burr. [Color figure can be viewed in the online issue, which is available at wileyonlinelibrary.com.]

Heat Affected Zone

Microscopic images from HAZ are shown in Figure 4. Figure 5 also shows the results of HAZ measurement. As these results show, due to the lower thermal focus, PE exhibits smaller HAZ in comparison with PS. Semi-crystalline polymers have higher thermal conductivity due to their structure that assists to decrease thermal focus.[15–17] When the generated heat is transmitted rapidly, the time for developing HAZ is not provided.[18]

As this figure also shows, HAZ increases by increase in power for both the polymers. The power plays key role on the heat generation in laser process. When the power increases, the amount of generated heat will increase. This is confirmed by

experimental measurement of generated heat during the laser cutting process. Figure 6 shows the thermal picture of several runs and represents the increase of input-heat to the workpiece by power increasing. Therefore, the result of higher input-heat will generate higher HAZ. For better clarity, the thermal behaviors of amorphous and semi-crystalline polymers were studied. Thermal conductivity, specific heat, and thermal diffusivity are important parameters which determine the thermal properties of these materials. Among them, the thermal diffusivity can be useful for better clarification of experimental observations. The PE samples have a higher thermal conductivity in comparison with PS but they have equal thermal diffusivity at 20 °C.[19,20] Thermal diffusivity α is defined as:

Table IV. Analysis of Variance of Burr Results

| Source	DF	Seq SS	Adj SS	Adj MS	F	P	P-effect	Statistical F
T	1	0.027028	0.027028	0.027028	14.02	0.005	15.54	5.12
P	3	0.129159	0.129159	0.043053	22.33	0.000	24.75	3.86
V	3	0.270459	0.270459	0.090153	46.76	0.000	51.82	3.86
$T \times P$	3	0.003009	0.003009	0.001003	0.52	0.679	0.58	3.86
$T \times V$	3	0.033659	0.033659	0.011220	5.82	0.017	6.45	3.86
$P \times V$	9	0.013653	0.013653	0.001517	0.79	0.637	0.87	3.18
Error	9	0.017353	0.017353	0.001928				
Total	31	0.494322			$S = 0.044$ R-Sq $= 96.49\%$ R-Sq(adj) $= 91.91\%$			
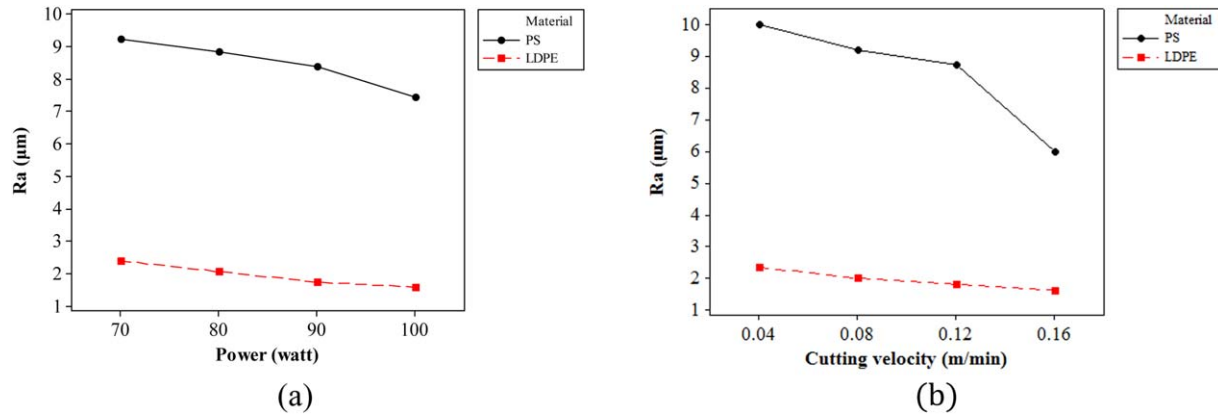
Figure 8. Influence of (a) power and (b) cutting velocity on R_a. [Color figure can be viewed in the online issue, which is available at wileyonlinelibrary.com.]

$$\alpha(T) = \frac{\lambda K(T)}{\rho \; C_p(T)} \tag{1}$$

where $K(T)$ is thermal conductivity, ρ is density and $C_p(T)$ is specific heat. On the other hand $C_p(T)$ is defined as:

$$C_p(T) = \left(\frac{\partial h}{\partial T} \right) \tag{2}$$

where h is enthalpy and T is temperature. For polymers thermal diffusivity is a function of temperature. When the temperature is increased by higher power, the thermal conductivity and specific heat will increase and subsequently thermal diffusivity will be decreased. By reduction of thermal diffusivity, the velocity of thermal transmission is diminished. This phenomenon slows the dissipation of generated heat and increases HAZ width.

Furthermore, the HAZ reduces by increase in cutting velocity. According to thermal measurement and results of previous researches, increase of cutting velocity reduces the contact time between workpiece and laser beam. Therefore, the input-heat will decrease that hinders the developing of HAZ.[18]

Table III displays the analysis of variance (ANOVA) for HAZ results. The calculated F values of three variable input parameters and interaction between material type and power are smaller than statistical F values. Therefore, they have a significant effect on HAZ. In addition, the highest percent effect

amount after material type pertains to cutting velocity that proves it as the most effective parameter on HAZ.

Burr

Effects of different parameters on burr height are shown in Figure 7. As can be seen, increasing of power decreases the burr amounts. In higher power, the viscosity of polymer decreases that causes to rapid void of melting material from the cut path.[17] The height of burr decreases when the melting material is swiftly removed from the kerf.

As seen in this figure, an inverse relationship exists between burr and cutting velocity for both the polymers. The increasing of cutting velocity accelerates the removal of materials that creates lower burr. Finally, it can be inferred that the increasing of power and cutting velocity provide the optimum conditions of cutting and reducing the burr.

Table IV represents the ANOVA of burr results. The comparison between calculated F values and statistical F amounts reveals that input parameters are the effective parameters. It can be also found that the interaction between material type and cutting velocity have a significant influence on burr. The obtained P-values confirm these findings. The percent effect of cutting velocity is 51.82 which shows the cutting velocity is the most important factor on burr.

Table V. Analysis of Variance of Surface Roughness Results

Source	DF	Seq SS	Adj SS	Adj MS	F	P	P-effect	Statistical F
T	1	341.781	341.781	341.781	6901.75	0.000	95.65	5.12
P	3	7.592	7.592	2.531	51.10	0.000	0.71	3.86
V	3	24.683	24.683	8.228	166.15	0.000	2.3	3.86
$T \times P$	3	1.256	1.256	0.419	8.46	0.006	0.12	3.86
$T \times V$	3	12.989	12.989	4.330	87.43	0.000	1.21	3.86
$P \times V$	9	0.311	0.311	0.035	0.70	0.700	0.01	3.18
Error	9	0.446	0.446	0.050				
Total	31	389.057			$S = 0.222533$ R-Sq = 99.89% R-Sq(adj) = 99.61%			
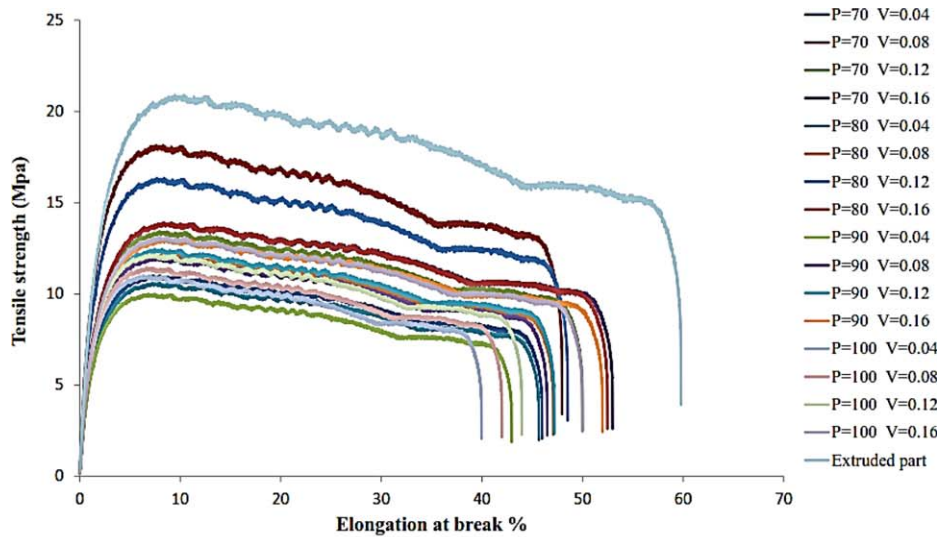
(a)
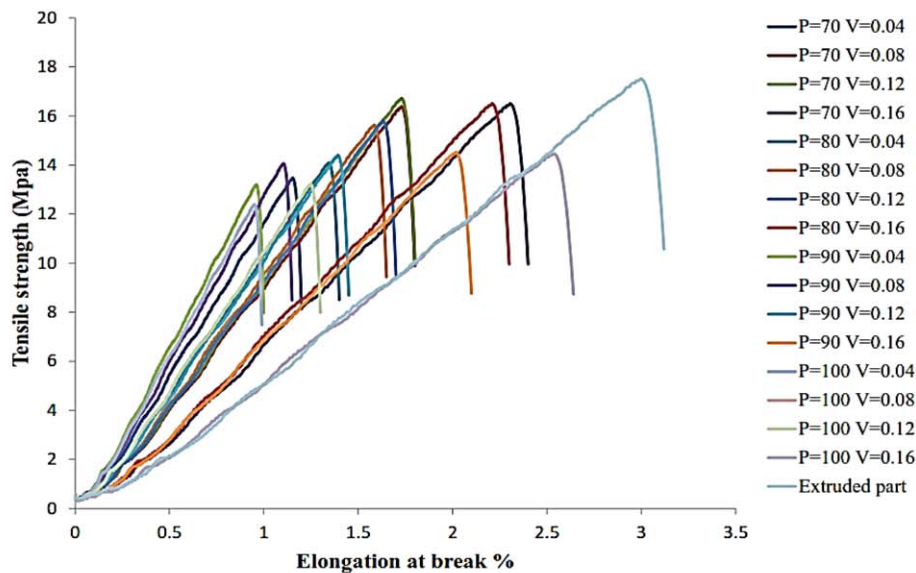
(b)

Figure 9. Elongation–stress curves for every run of experiments: (a) LDPE and (b) PS. [Color figure can be viewed in the online issue, which is available at wileyonlinelibrary.com.]

Surface Roughness

Figure 8 depicts the effect of power and cutting velocity on the surface roughness. Inequality of results can be seen for two polymers. The samples of PS were produced rougher than PE samples. It seems the lower thermal conductivity results in rapid solidification of melted layer on the surface and formation of an aggravated surface condition.

According to Figure 8, the higher power and cutting velocity has a slight effect on the improvement of surface roughness. In the case of PS, the microscopic studies proved that the higher power and cutting velocity generate less sink marks and remnant spots on the surface and also decrease surface roughness. For PE samples, it was also observed that the increase in power and cutting velocity are equally important factor in order to improve the structure of cut surface of samples. These observations can be attributed to the viscosity. As it has been described, increasing of temperature (by higher power) decreases the viscosity of polymer in the cutting process. Lower viscosity helps to void melting material from the kerf and also decreases the adhesion of melted material by side edge and surface. On the other hand, higher cutting velocity also cooperates to quick void of kerf from the melted material.

Figure 10. The specimens after tensile test.

Table V represents the ANOVA of surface roughness results. Accordingly, all of the input variables and interactions between them are statistically effective on the R_a at the 95% confidence level excluding power $\times$ cutting velocity, which is not effective parameter on surface roughness of the samples. According to P-effect values, after type of material, the cutting velocity is the

second effective parameter on surface roughness. This result shows cutting velocity is more effective than power on R_a.

Mechanical Properties

Figure 9 illustrates the tensile curves for every run of examinations. In order to compare the tensile strength of the samples produced by laser cutting and extruded sheet, the samples were prepared by common mechanical cutter and tested. As it is obvious in Figure 9, the tensile strength reduced after laser cutting. Figure 10 represents the samples after tensile tests. Figure 11 also shows the effect of laser parameter on tensile strength and elongation at break. It is observable that the power and cutting velocity have the same effect on two polymers. The decreasing of tensile strength and elongation at break by increase in power is a remarkable finding. On the other hand, these parameters are improved by cutting velocity.

The reasons of tensile strength alternation can be searched in three points: HAZ, microcracks, and surface roughness. The increase of temperature in HAZ deteriorates the polymer structure in this area and decreases its strength. In general view, the HAZ is not accounted as influential area from samples under the tensile loads. Based on results, increasing of power and decreasing of cutting velocity develop the width of HAZ and consequently have a deteriorating effect on the tensile strength.
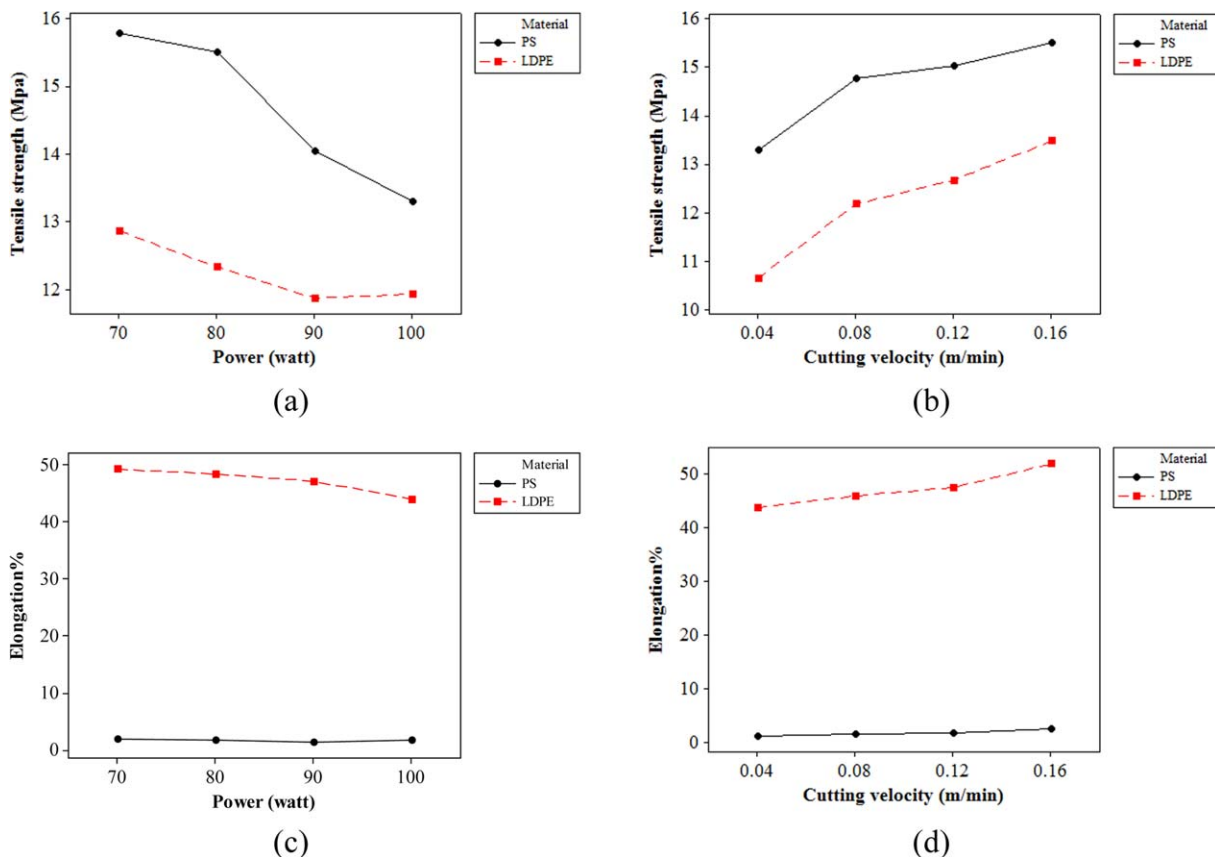

Figure 11. Effect of (a,c) power and (b,d) cutting velocity on tensile strength and elongation at break. [Color figure can be viewed in the online issue, which is available at wileyonlinelibrary.com.]

Table VI. Analysis of Variance of Tensile Strength Results

Source	DF	Seq SS	Adj SS	Adj MS	F	P	P-effect	Statistical F
T	1	46.4451	46.4451	46.4451	462.22	0.000	74.29	5.12
P	3	15.4010	15.4010	5.1337	51.09	0.000	8.21	3.86
V	3	27.3836	27.3836	9.1279	90.84	0.000	14.6	3.86
$T \times P$	3	3.9835	3.9835	1.3278	13.21	0.001	2.12	3.86
$T \times V$	3	0.4926	0.4926	0.1642	1.63	0.249	0.26	3.86
$P \times V$	9	2.8703	2.8703	0.3189	3.17	0.05	0.51	3.18
Error	9	0.9043	0.9043	0.1005				
Total	31	97.4805		$S = 0.316989$ R-Sq $= 99.07\%$ R-Sq(adj) $= 96.80\%$				

The microcracks are the second reason. HAZ has a potential to grow the present microcracks on the surface and also in the boundary line between HAZ and polymer matrix. The microscopic images (Figure 10) confirm that when the samples are exposed to the tensile load, these microcracks grow and finally lead to fracture.

The surface roughness is the third reason for explaining the variation of tensile strength. As it has been described, in the case of surface roughness, cutting velocity is more effective than power. Therefore, increasing of tensile strength by increase in cutting velocity can be attributed to better surface quality. The rough surface has a negative effect on mechanical properties. When a sample with rough surface is exposed to tensile load, the stress is concentrated in roughness points, resulting in stress concentration and fracture of sample loads below the strength levels.[21] Improvement of surface roughness can be also influential on shaped cracks. According to microscopic studies, the number of cracks on the smooth surfaces is lower. So, higher tensile strength can be observed for parts by lower surface roughness.

The AVNOVA result of tensile strength's data is tabulated in Table VI. It is observed that for tensile strength all of considered parameters are effective excluding the interaction between materials and cutting velocity. Regarding the P-effect amounts, the cutting velocity is more effective than power. The effect of interaction between power and cutting velocity is another noticeable factor that can be seen.

As described earlier, tensile strength is a direct function of HAZ and surface roughness. In order to predict the tensile strength of parts after laser cutting process, two separate and individual mathematical models based on regression are presented in Table VII for LDPE and PS.

Where R_a (µm) is surface roughness, HAZ (mm) is the heat affected zone, A_0 (mm^2) is cross-section of specimen. The σ_0

(Mpa) is also tensile strength of base polymeric material before laser cutting.

CONCLUSIONS

Microscopic and mechanical properties of crystalline (LDPE) and amorphous (PS) polymeric parts after laser cutting process were examined. The acquired results showed that:

The microcracks, re-solidified spots of molten material and sink marks appear on the cut surface of amorphous polymer but they are not present on the crystalline polymer. The microcracks were also observed in three areas: cut surface, HAZ, and boundary of HAZ with base polymer.

The HAZ and surface roughness amounts are smaller for semi-crystalline polymer. The laser input parameters have similar effects on HAZ and surface roughness for both polymers. Decreasing of power and increasing of cutting velocity reduce the HAZ and surface roughness.

Tensile strength of semi-crystalline and amorphous polymers reduced after laser cutting. Creation of HAZ and roughening of the surface are the reasons which diminish the tensile strength. Developing of HAZ and reduction of surface quality by increasing of power and decreasing of cutting velocity are the main factors which deteriorate the tensile strength of samples. Moreover, in the case of amorphous polymer, the presence of microcracks in HAZ plays key role on its tensile strength. According to microscopic studies, these microcracks grow under the tensile load and eventually result in fracture of the sample under the original tensile strength of base polymer. Finally, lower power and higher cutting velocity should be recommended for achieving better tensile strength.

REFERENCES

1. Powell, J. CO$_2$ Laser Cutting; Springer-Verlag: Berlin, Germany, Vol. *214*, **1993**.

2. Webb, C. E.; Jones, J. D. Handbook of Laser Technology and Applications: Laser Design and Laser Systems; CRC Press: Boca Raton, USA, **2004**.

3. Eltawahni, H.; Hagino, M.; Benyounis, K.; Inoue, T.; Olabi, A. G. *Opt. Laser Technol.* **2012**, *44*, 1068.

Table VII. Mathematical Model for Prediction of Tensile Strength after Laser Cutting

$\sigma_{UTS} = 0.018242 \cdot \sigma_0 \cdot \left(A_0 - \left(HAZ + \frac{Ra}{1000}\right)\right)$	(3)	PS
$\sigma_{UTS} = 0.018291 \cdot \sigma_0 \cdot \left(A_0 - \left(HAZ + \frac{Ra}{1000}\right)\right)$	(4)	LDPE

4. Ready, J. F.; Farson, D. F.; Feeley, T. LIA Handbook of Laser Materials Processing; Laser Institute of America: Orlando, **2001**.

5. Migliore, L. R. Laser Materials Processing; CRC Press: Boca Raton, USA, **1996**.

6. Caiazzo, F.; Curcio, F.; Daurelio, G.; Minutolo, F. M. C. *J. Mater. Process. Technol.* **2005**, *159*, 279.

7. Shin, Y.; Kim, Y.; Park, S.; Jung, B.; Lee, J.; Nelson, J. S. *J. Laser Appl.* **2005**, *17*, 243.

8. Davim, J. P.; Barricas, N.; Conceicao, M.; Oliveira, C. *J. Mater. Process. Technol.* **2008**, *198*, 99.

9. Davim, J. P.; Oliveira, C.; Barricas, N.; Conceição, M. *Int. J. Adv. Manuf. Technol.* **2008**, *35*, 875.

10. Choudhury, I.; Shirley, S. *Opt. Laser Technol.* **2010**, *42*, 503.

11. Niino, H.; Harada, Y.; Anzai, K.; Matsushita, M.; Furukawa, K.; Nishino, M.; Fujisaki, A.; Miyato, T. *J. Laser Micro Nanoeng.* **2016**, *11*, 104.

12. Ghavidel, A. K.; Azdast, T.; Shabgard, M.; Navidfar, A.; Sadighikia, S. *J. Appl. Polym. Sci.* **2015**, *132*, DOI: 10.1002/app.42671.

13. Lootz, D.; Behrend, D.; Kramer, S.; Freier, T.; Haubold, A.; Benkiesser, G.; Schmitz, K. P.; Becher, B. *Biomaterials* **2001**, *22*, 2447.

14. Herzog, D.; Jaeschke, P.; Meier, O.; Haferkamp, H. *Int. J. Mach. Tools Manuf.* **2008**, *48*, 1464.

15. Crawford, R.; Crawford, R. J. Plastics Engineering; UK, Oxford. Butterworth-Heinemann,**1998**.

16. McKeen, L. W. Effect of Temperature and Other Factors on Plastics and Elastomers, The PDL Handbook Series; Norwich, NY, UK. Elsevier Science & Technology, **2007**.

17. Rao, N.; O'Brien, K.; Rao, N.; O'Brien, K. *Design Data for Plastics Engineers;* **1998**.

18. Ghavidel, A. K.; Azdast, T.; Shabgard, M. R.; Navidfar, A.; Shishavan, S. M. *Opt. Laser Technol.* **2015**, *67*, 119.

19. Rao, N. S. Design Formulas for Plastics Engineers; Carl Hanser Verlag: Germany, **1991**; Vol. *1991*, p 135.

20. Ogorkiewicz, R. M. Thermoplastics: Properties and Design; Hoboken, New Jersey, United States, Wiley, **1974**.

21. Joslin, D.; Oliver, W. *J. Mater. Res.* **1990**, *5*, 123.